



# Laboratory Measurement of Permeability Evolution Behaviors Induced by Non-Sorbing/Sorbing Gas Depletion in Coal Using Pulse-Decay Method

Peng Liu<sup>1,2</sup> · Jinyang Fan<sup>1,2</sup> · Deyi Jiang<sup>1,2</sup>

Received: 9 February 2021 / Accepted: 25 August 2021 / Published online: 4 September 2021  
© The Author(s), under exclusive licence to Springer Nature B.V. 2021

## Abstract

Gas permeability in coal plays a critical role in predicting coalbed methane (CBM) production. The permeability evolution induced by gas depletion in low-permeability coal is complicated and affected by multi-mechanistic flow components. This study runs a series of permeability tests using the pulse-decay method for helium and CH<sub>4</sub>, CO<sub>2</sub> depletions in coal under both the constant stress boundary (CSB) and uniaxial strain boundary (USB) conditions. With the measured pulse-decay curves, the gas desorption effect on pore pressure depletion can be clearly noticed and gas permeability change can be estimated. The result shows that the helium permeability under the CSB condition is slightly lower than that under the USB condition, and it decays nonlinearly with pressure drawdown and does not rebound in the low-pressure region, which indicates that the helium permeability evolution is mainly controlled by the effective stress in the tested coal. For the sorbing gas CH<sub>4</sub>/CO<sub>2</sub>, the permeability profile under the two boundary conditions behaves somewhat similarly; it initially declines with the pressure depletion and then starts to rebound in low-pressure region. The permeability ‘rebound’ of CH<sub>4</sub> is comparatively less than that of CO<sub>2</sub> due to the larger adsorption capacity of CO<sub>2</sub> in coal. With the comparison of permeability behaviors of the different test fluids, it is inferred that the sorbing gas permeability ‘rebound’ should be mainly caused by the matrix shrinkage. The result of this study reveals that coal reservoirs produce CBM using a multi-mechanism approach, and the effect of matrix flows on the permeability behavior and the overall CBM production should be highly emphasized.

**Keywords** Coal permeability test · Pulse decay method · Gas permeability evolution · Uniaxial strain

---

✉ Peng Liu  
rocliu@cqu.edu.cn

<sup>1</sup> State Key Laboratory of Coal Mine Disaster Dynamics and Control, Chongqing University, Chongqing 400030, China

<sup>2</sup> College of Resources and Safety Engineering, Chongqing University, Chongqing 400030, China

## 1 Introduction

Coalbed methane (CBM), as a natural formed gas stored in coal reservoirs, is an emerging unconventional energy source with possible greenhouse gas effects (Moore 2012; Palmer 2010; Ritter et al. 2015; Cheng and Pan 2020). Besides, it is a 'mineral bane' that makes the mining process more dangerous. Given their distinct economic prospect, CBM development and CO<sub>2</sub> sequestration in coal have been gaining more interest worldwide (Liu et al. 2018a; Liu et al. 2020a; Fan et al. 2020). As a result, there has been a growing research activity at the academic and industrial levels, which has provided an opportunity for promoting mine safety, increasing the energy supply and reducing the damages on the environment (Liu et al. 2021).

For a porous medium, permeability is a critical property that assesses the capacity of the medium to conduct or transmit fluids (Wu et al. 2020; Wang and Liu 2016; Liu et al. 2020a). The gas permeability of coal is intensively related to the medium flow behavior within coal (including gas depletion or CO<sub>2</sub> injection for the purposes of sequestration or enhanced recovery) and has been fully analyzed in multiple CBM studies (Palmer 2009; Ma et al. 2011; Liu et al. 2012; Pan and Connell 2012; Shi and Durucan 2005; etc.). In the view of engineering practices, CBM production rate and injecting CO<sub>2</sub> for enhancing CBM recovery are mainly controlled by the gas permeability of coal reservoir and its dynamic behaviors with pore pressure depletion (Liu et al. 2010, 2016; Perera et al. 2012; Zang et al. 2020).

## 2 Background and Previous Studies

Permeability is an inherent property that defines how readily fluid flows in a porous media (Liu et al. 2012; Pan and Connell 2012; Liu and Harpalani 2013). With extensive field observations and laboratory studies on coal gas interaction, it was observed that coal permeability can vary dynamically during gas depletion/injection as a response to two competitive actions: matrix shrinkage/swelling induced by gas ad/desorption and mechanical expansion/compression of solid coal due to pressure injection/depletion in pores (Levine 1996; Robertson 2005; Harpalani and Mitra 2010; Mitra 2010).

### 2.1 The Dual-Porosity Concept of Coal Structure

Gas bearing coal is a porous media, consisting of a primary and secondary porosity systems for gas storage and transportation, and has the characteristics of dual porosity, low permeability and water-saturated (Liu et al. 2020b; Peng et al. 2017). The primary porosity system (matrix system, as shown in Fig. 1) is the major location for adsorbed gas which accounts for the great majority of the total gas content in coal (Zhang et al. 2016; Crosdale et al. 1998). The fracture network serves as the secondary porosity system (as shown in Fig. 1), which provides the fluid (including gas and water) flow path in coal (Fan et al. 2020). For modeling gas storage and transport in coal reservoirs, the matchstick model was proposed by Seidle et al. (1992) to represent the geometry of ordinary natural coal reservoir. Each matchstick refers to a coal matrix and the apertures between the matrixes correspond to the fractures, as shown in Fig. 1.

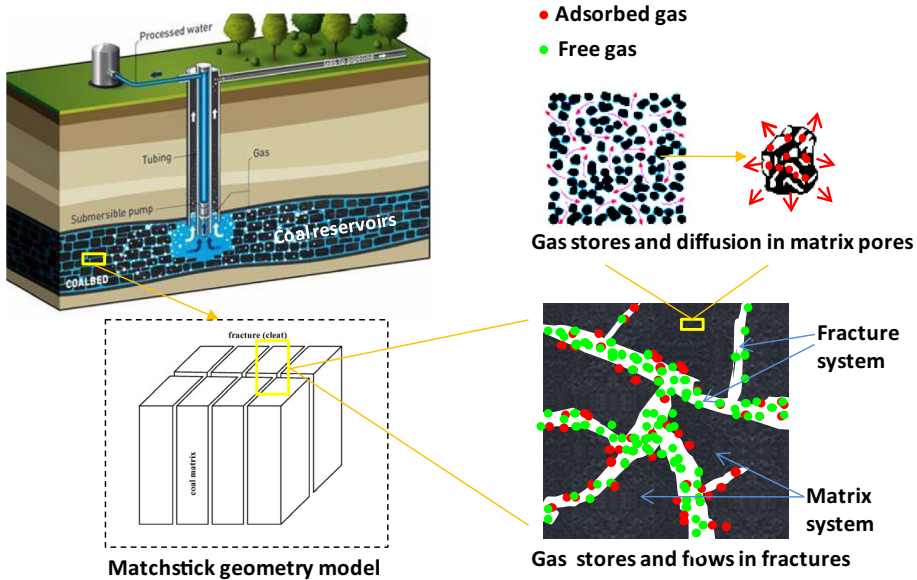


Fig. 1 Illustration of coal structure

## 2.2 Theoretical Studies of Coal Permeability

During pore gas pressure depletion, gas desorption and diffusion from coal matrix lead to matrix deformation shrinkage, which will increase the aperture of coal fracture and promote the fracture permeability. Because the effects of matrix deformation and effective stress change influence cleat apertures, it can be concluded that gas permeability coal reservoir changes over the entire gas depletion process. A significant effort has been devoted to describing coal permeability evolution induced by the aforementioned mechanism during coal–gas interaction. Numerous analytical permeability models have been proposed for understanding and simulating coal gas interaction behavior.

Gray (1987) considered the change of effective stress and coal matrix deformation induced by gas desorption and proposed one of the first coal permeability models. Sawyer et al. (1990) studied the relation of coal matrix compressibility and the gas sorption behavior, and indicated that coal matrix shrinkage could balance the partial volume compaction of coal fracture caused by the effective stress increase. Seidle et al. (1992) applied the matchstick assumption of coal mass and derived a permeability model with the hydrostatic stress and matrix shrinkage considered. Harpalani and Chen (1995) proposed a permeability model with the assumption of the matchstick geometry and coal swelling in a constant volume. Levine (1996) pointed out that the new cleat aperture width was not changed because the fracture compaction closed the fracture aperture and matrix shrinkage opened fracture width. Palmer and Mansoori (1996) assumed the uniaxial strain condition to replicate the in situ condition and derived a popular permeability model linking the permeability change with the variation of gas pressure and stress on coal. Based on the Seidle et al.’s model, Shi and Durucan (2004) built a modified permeability model with the assumption that permeability has an exponential relationship with the horizontal effective stress. Cui

and Bustin (2005) considered the linear poroelasticity and coal swelling, and derived a model to resolve the permeability change with the stress variation in coal. Liu and Rutqvist (2010) assumed fracture retained some opening under infinitely high stress loaded and built a model linking the stress and permeability change. Pan and Connell (2011) considered the anisotropic characteristics of coal permeability and developed a permeability model to resolve the anisotropic swelling behavior of coal and gas permeability evolution. Based on the stress–strain relationship and the S&D model, Liu et al. (2012) considered the isothermal gas desorption process to calculate the matrix shrinkage deformation and proposed a permeability model under the uniaxial strain condition. After that, based on these permeability models abovementioned, many other scholars proposed dynamic permeability models involving the stress condition, matrix shrinkage and gas slippage and other factors (Wang et al. 2014; Durucan et al. 2014; Chen et al. 2016; Niu et al. 2018; Wang et al. 2018).

### 2.3 Laboratory Studies of Coal Permeability Test

Besides the theoretical studies related to the permeability evolution, many experimental works has been conducted to obtain laboratory permeability data, which also can be used to verify the permeability evolution model. For the coal permeability tested in the laboratory, two approaches are commonly used: the transient-state method and the steady-state method (Feng et al. 2019). The root of the two approaches is the Darcy's law, which is commonly applied in estimating the permeability value in porous rock and coal with the experimental data.

In order to understand the permeability change in coal, multiple laboratory tests have been conducted and presented in the previous literature. Harpalani and McPherson (1985) measured the gas permeability of coal under various stress conditions and indicated that the logarithm of permeability value was linearly related to the hydrostatic stress. Durucan and Edwards (1986) suggested that stress loaded on coal will lead to the pores compression and coal fracture development and then change gas permeability of coal. Based on the observation that permeability decreased first and then increased sharply under constant hydrostatic stress conditions, Harpalani and Schraufnagel (1990) observed the permeability rebound when gas desorption prevails significantly. Harpalani and Chen (1997) experimentally studied the coal permeability change affected by the gas slippage effect and matrix volumetric strain and observed a permeability increase with the pressure depletion in low-gas-pressure stage. Pan et al. (2010) investigated the effect of strain changes on the porosity and permeability of coal and found that the adsorption induced coal swelling dominated the permeability change under confining stress conditions. Mitra et al. (2012) studied the permeability of coal core under the uniaxial strain condition, which was the first test of its kind to replicate the real condition of in situ coal reservoir. Liu (2012) observed that gas permeability in coal changes in a nonlinear pattern with pressure depletion, and an increasing trend of permeability evolution may appear when the reservoir pressure falls below a certain level. Feng et al. (2016, 2017) applied the pulse decay method to test the gas permeability of coal and indicated that the effective horizontal stress significantly affected the gas permeability behavior, and increasing the horizontal stress will have a negative impact on the permeability variation.

### 3 Summary of the Previous Studies

Among the existing permeability models, most of which are developed with the assumption of uniaxial strain condition, it is assumed that the constant vertical stress and zero horizontal strain are used to replicate the in situ condition (Gray 1987; Palmer and Mansoori 1996; Pekot and Reeves 2003; Cui and Bustin 2005; Shi and Durucan 2005; Ma et al. 2011; Mitra et al. 2012; Liu et al. 2012; Liu and Harpalani 2014a; etc.). A few models are derived based on the boundary conditions of constant confining stress, defined as both the unchanged confining stress and the unchanged vertical stress. This was most widely used in permeability laboratory tests (Robertson 2005; Liu and Rutqvist 2010; Chen et al. 2012). It should be noted that the measured data used for model validation depends on the stress boundary under which the model is derived; otherwise, it may lead to significant errors. Coal permeability tests are normally carried out with the constant stress boundary (Robertson 2005; Chen et al. 2012; Liu and Rutqvist 2010; Pini et al. 2009), while some tests are conducted under uniaxial strain conditions (Mitra et al. 2012; Liu and Harpalani 2014). With the uniaxial strain boundary conditions, the lateral stress should be maintained dynamically changing to ensure zero lateral strain, which is comparatively difficult to achieve than keeping constant confining stress condition (Liu et al. 2010; Connell 2016; Mitra et al. 2012). Different boundary settings lead to different stress profile in coal and also result in different permeability behaviors. Therefore, the inconsistency between the experimental boundary conditions and model assumptions implies that it should be undertaken cautiously to validate permeability models obtained from measured data or to interpret the experimental permeability performance based on the analytical model. On the other hand, most of laboratory tests for gas permeability in coal applied the steady-state methods, and it requires the stability of pressure and gas flow flux during the steady-state test process, which will take a long time to stabilize the pressure and flow in the cylindrical coal core. Therefore, using the steady-state method to test low-permeability coal will be quite time-consuming. The transient method has the advantages of fast and efficient on permeability testing, but its application is not much in measuring the coal permeability.

In the current study, a series of pulse decay tests for gas permeability and its evolution induced by both non-sorbing and sorbing gases depletion under the constant stress and uniaxial strain conditions was carried out. Then the gas permeability was estimated using the pulse decay curves, and the permeability alteration induced by pore pressure change in coal and the related interpretations were reported. The study aimed at analyzing the permeability performance using laboratory tests and promoting the understanding of the permeability evolution behavior during coal gas interaction.

## 4 Experimental Work

### 4.1 Experimental Setup

This study employed the ‘pulse-decay’ method to test the gas permeability in coal (Brace et al. 1968; Wang et al. 2015). The ‘pulse-decay’ method is a transient-state method derived based on Darcy’s law, in which the pressure gradient between the upstream and downstream of a coal sample was initially created, and then, the pulse-decay responses during test duration were recorded and used to permeability estimation (Feng et al. 2019).

The experimental setup was designed to implement the measurement of permeability and its evolution induced by gas pressure drawdown under the constant stress condition and the uniaxial strain condition. The experiment system mainly consisted of a gas flow system, a stress loading system and a data collection system, as shown in Fig. 2. The temperature was kept constant at 308 K throughout the entire measurements. The syringe pumps are capable of changing or maintaining axial/lateral stresses to the desired stress values. The pressure data were monitored and recorded by the installed high-accuracy pressure transducer and data acquisition device during the experiment process. This study firstly conducted the permeability tests under the constant stress condition followed by the uniaxial strain condition. Both the non-sorbing gas (helium, He) and the sorbing gas ( $\text{CH}_4$ ,  $\text{CO}_2$ ) were used as the test fluids.

## 4.2 Sample Preparation

The coal samples for the permeability test were collected from an ultra-tight coal reservoir located in the Illinois Basin. Cylindrical coal cores ( $\sim 25$  mm in diameter) were drilled from the coal blocks; the two ends of the cylindrical core were trimmed to  $\sim 50$  mm in length. After the preparation, the sample cores were placed in an environmental chamber to prevent weathering and keep the moisture content constant until being placed in the triaxial cell.

## 4.3 Experimental Procedure

The permeability measurement was taken under two different boundary conditions: the constant stress condition and in situ/uniaxial strain condition. During the permeability tests, the coal core was loaded in the triaxial cell and gradually stressed to 13.8 MPa for the

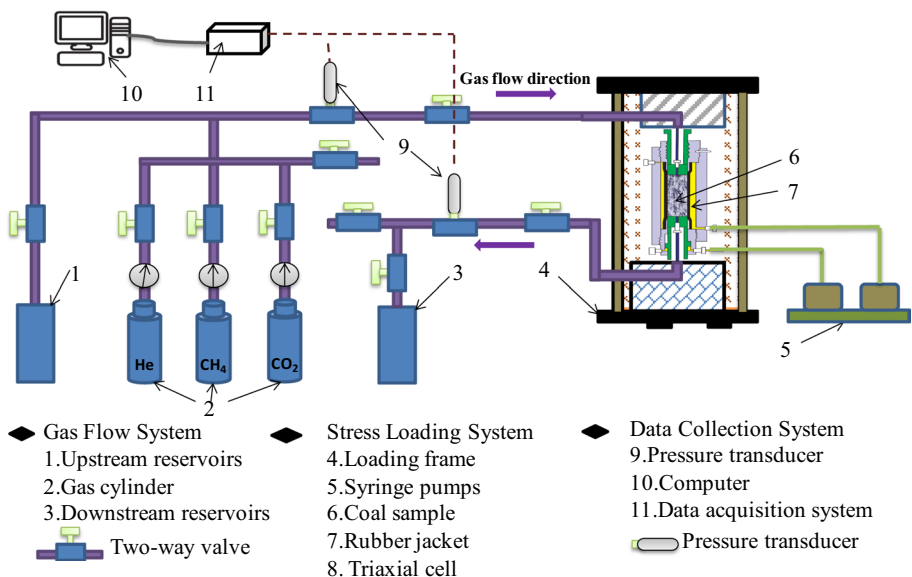


Fig. 2 Schematic of experimental setup

axial stress; hydraulic oil was injected into the triaxial cell to create an either constant or a changing confining stress on coal core.

### 4.3.1 Permeability Tests Under Constant Stress Boundary

Helium was chosen initially as the fluid medium to estimate the permeability evolution, and then, CH<sub>4</sub> and CO<sub>2</sub> were also used. The coal sample was loaded in the triaxial cell and gradually stressed to 6.9 MPa for the confining stress. While reaching the mechanical equilibrium, the residual air in the experiment system was degassed using a vacuum pump. Gas depletion was applied to replicate the in situ gas extraction procedure. Helium was then injected at 4.15 MPa for both the upstream and downstream. After attaining the equilibrium, the gas pressure for downstream was reduced 4 MPa, subsequently creating a pressure gradient ~0.15 MPa between the upstream and downstream of the coal core. Following this, the valve between the coal sample and the downstream was opened, so the fluid medium was able to flow through the sample downstream. The pressure response in up-/downstream over time was recorded to estimate the permeability. To mimic the gas depletion, stepwise depletions were conducted with similar pressure interval, and the final equilibrium pressure (around 0.2 MPa) was obtained with the designed six pulse decay tests. Throughout the test duration, both the vertical and the confining stress are maintaining constant. After finishing the helium cycle, similar depletion steps were carried out with CH<sub>4</sub> and CO<sub>2</sub> for sorbing gas permeability measurements. The gas permeability corresponding to each pressure step could be estimated based on the pressure data. This was the gas depletion procedure under the constant stress condition; after that, the permeability gas depletion was tested under the in situ boundary.

### 4.3.2 Permeability Tests Under Uniaxial Strain Boundary

The vertical/axial stress was initially loaded at 6.9/13.8 MPa. For the in situ/uniaxial strain boundary, the lateral stress was passively adjusted with gas depletion to maintain the zero lateral strain. To achieve the in situ boundary condition, the volume of hydraulic oil injected into the triaxial cell was continuously changed to adjust the confining stress and ensure the zero lateral strain, and the volume change of hydraulic oil was also monitored and record to estimate the lateral stress change. Similar to the tests under the constant stress boundary, the gas pressure of the tested sample was depleted from ~4.15 MPa with a pressure gradient ~0.15 MPa while maintaining a uniaxial strain condition. Helium, CH<sub>4</sub> and CO<sub>2</sub> were used sequentially to flow through the coal sample, and the permeability values for all tested gases at each pressure step were estimated.

For the permeability tests, the pore pressure in coal core depleted from ~4.15 MPa to around 0.2 MPa with a stepwise way, and five pulse decay tests were conducted under each boundary condition for helium, CH<sub>4</sub> and CO<sub>2</sub>. Gas permeability values corresponding to different gas pressures and boundary conditions can be estimated by the pulse decay data recorded during the test duration.

## 4.4 Permeability Estimation with the Pulse-Decay Data

The pulse decay technique provides an effective approach to measure the permeability and its change behavior in ultra-tight/tight coal. Brace et al. (1968) derived the pressure



transient equation (shown in Eqs. (1) and (2)) to calculate the permeability based on the measured pulse-decay pressure curves.

$$p_u(t) - p_d(t) = [p_u(t_0) - p_d(t_0)]e^{-\alpha t} \quad (1)$$

$$\alpha = \frac{kA_s}{\mu L c_g} \left( \frac{1}{V_u} + \frac{1}{V_d} \right) \quad (2)$$

where  $p_u(t)$  and  $p_d(t)$  are the gas pressures for the up-/downstream of the coal core;  $t_0$  means the initial time value;  $\alpha$  means the slope of the pressure–time curve over time on semilog figure;  $A_s$  is the cross-sectional area of the tested coal core;  $\mu$  is the gas viscosity;  $L$  indicates the sample length;  $c_g$  indicates gas compressibility; and  $V_u$  and  $V_d$  are volumes of the upstream/downstream reservoir. The permeability  $k$  can be estimated with the pressure data measured in the experiments.

## 5 Results and Discussion

### 5.1 Approaches to Measure the Gas Permeability in Low-Permeability Coal

The steady-state method is the most commonly used method for experimentally determining coal permeability, because of its simplicity for understanding and interpretation the measured data (Feng et al. 2017). In the steady-state permeability tests, the gas permeability of the tested coal is estimated by measuring the gas pressure and gas flow of the upstream and downstream of the coal core (Harpalani and Chen 1997). The steady-state method requires that the pressure and flow of the coal sample should be stable before and after the experiment. In general, columnar cores are normally used for experimental coal samples, and it takes a long time to stabilize the pressure and flow. Therefore, the steady-state experimental method could be very time-consuming. Moreover, the gas permeability of coal samples and other rocks from the ultra-tight/tight reservoirs are extremely low, and the gas flow rate is usually quite small. Accurate flow measurement requires a highly accurate flow meter, which increases the difficulty and error of steady-state experiments. Thus, the steady-state experimental method is not applicable to measure the low permeability in rocks. The pulse-decay method was originally used to determine the permeability of tight rocks, but it has only recently been applied to coal permeability determination experiments. Such experimental methods are mainly reported in research papers by scholars (Brace et al. 1968; Pini et al. 2009; Mitra 2010; Feng et al. 2016, 2017). Compared with the steady-state method, the pulse-decay method only needs to measure the gas pressure data of the up-/downstream of the tested coal core, and estimate the permeability based on the pulse decay curve. Therefore, the pulse decay method is believed to be better suited for characterizing gas permeability of coal and its change behaviors in ultra-tight/tight coal.

### 5.2 Pulse-Decay Curve of He, CH<sub>4</sub> and CO<sub>2</sub>

Many previous works have proved that the gas permeability in porous coal is very gas-dependent, and the permeability behavior using different experimental gases is different for the same coal core. Also, it is observed that the adsorption/diffusivity property in coal is gas type-dependent. Because CO<sub>2</sub> has smaller kinetic diameter and higher



adsorption affinity than  $\text{CH}_4$ , it will have a larger ad-/desorption capacity in coal than  $\text{CH}_4$ . Therefore, under the same condition,  $\text{CO}_2$  depletion in coal will lead to a more significant volumetric strain of coal matrix (matrix shrinkage effect) than  $\text{CH}_4$ , which will have a greater impact on permeability. In the case of the non-sorbing gas helium, there is no volumetric strain induced by gas depletion. Therefore, volumetric strains of the coal matrix caused by pressure depletion with different permeating gases are different and thus lead to various behaviors of the permeability in coal. Besides, the gas permeability is affected by the Klinkenberg effect or slip flow in the pores of coal. The Klinkenberg coefficient is a parameter that quantifies the effect of the slip flow on permeability and is intently related to the gas molecular size and its mean free path. The gas molecular size and the mean free path are also different for different gases. Thus, the Klinkenberg effect of different gases in a same porous media is different, which will affect the evolution of permeability to various extents. In summary, the volumetric strain and Klinkenberg effect resulting from pressure depletion with different gases are different; the permeability evolution behavior during the depletion processes will vary depending on the permeating gas. Therefore, diverse permeability values will be obtained in the coal permeability tested with different gases ( $\text{He}$ ,  $\text{CH}_4$  and  $\text{CO}_2$ ).

Figure 3 shows the measured pulse-decay pressure response curves corresponding to variation pressure steps for  $\text{He}$ ,  $\text{CH}_4$  and  $\text{CO}_2$  under the constant stress boundary conditions. Because of the extremely long equilibrium time for low-pore-pressure steps, achieving equilibrium may consume more than 10 days at 0.84 MPa gas pressure; we only took a part of the entire pulse-decay curve to estimate the permeability, which significantly reduces the time of permeability testing. This is an advantage of the pulse-decay method as it helps relieve the time-consuming operation of permeability measurement for tight/ultra-tight rock.

Figure 3 shows that the pressure equilibrium time increases with the decrease in the injection pressure for all the tested fluids ( $\text{He}$ ,  $\text{CH}_4$  and  $\text{CO}_2$ ). For the non-sorbing gas helium, the permeability evolution is mainly determined by the effective stress effect in coal and the gas slippage effect, which is expected to decrease with the increase in the pore pressure due to the constant external stress, consequently giving rise to the permeability. For the sorbing gas ( $\text{CH}_4$  and  $\text{CO}_2$ ), coal deformation is mainly determined by the effective stress change and matrix shrinkage induced by gas desorption/diffusion from coal matrix. Additionally, gas slippage effect will become significant with the decrease in the pore pressure, manifested as varying degrees increase in the apparent permeability for the sorbing/non-sorbing gases in low-pressure range. Therefore, permeability evolution for sorbing gas is expected to be driven by multiple mechanisms and will display different variation trends compared to non-sorbing gas.

As observed in Fig. 3, the time required to approach the equilibrium for sorbing gas is generally more than that of helium gas, which physically indicates that sorbing gases tested here flow slower than non-sorbing through the same pore medium under similar conditions. For example, the durations required to complete all the pulse-decay steps for the three gases are 590 min, 780 min and 1300 min, respectively. When the pseudo-equilibrium pressure is about 0.88 MPa, the equilibrium times of  $\text{He}$ ,  $\text{CH}_4$  and  $\text{CO}_2$  are 220 min, 265 min and 400 min, respectively. With the comparison results, it is reasonable to conclude that much more time is required for sorbing gas than for non-sorbing gas to flow through the same coal under similar boundary conditions. This indicates that sorbing gases tested here flow slower than non-sorbing in the same conditions. Helium gas permeability is higher than the  $\text{CH}_4$  and  $\text{CO}_2$  gas permeability in coal, and similarly,

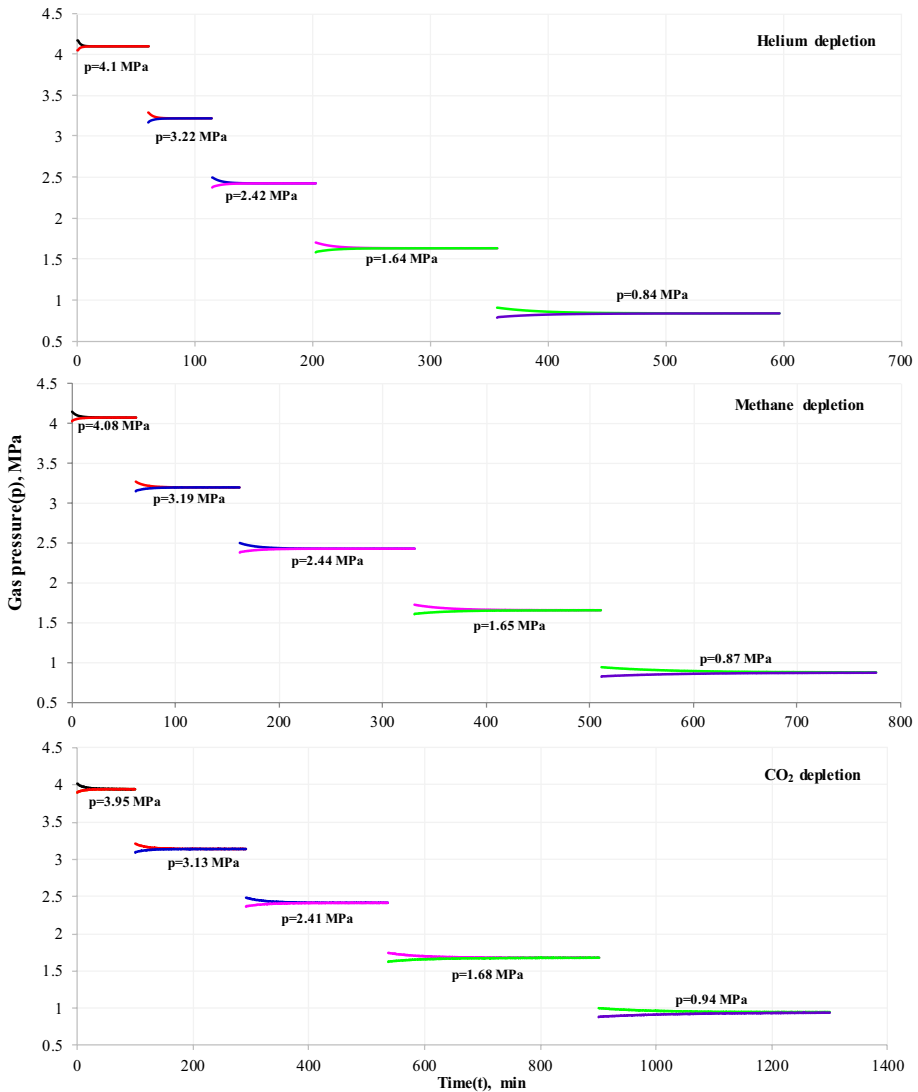


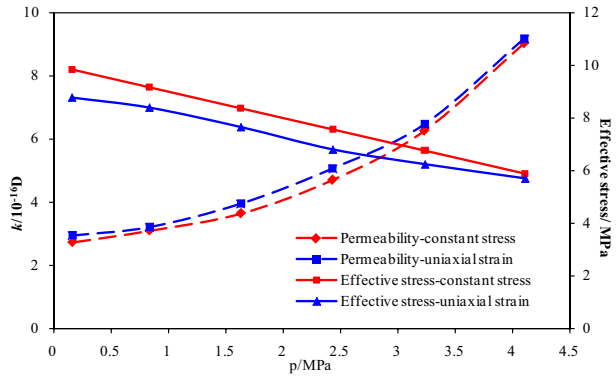
Fig. 3 Pulse-decay curves of pressure responses for He, CH<sub>4</sub> and CO<sub>2</sub> in gas depletion

the permeability of CH<sub>4</sub> gas in coal is lower than that of CO<sub>2</sub> gas. It also implies that coal permeability is a gas type-dependent property.

### 5.3 Helium Gas Permeability

Figure 4 shows the variation of the effective horizontal stress and helium gas permeability under the CSB and USB boundary conditions. As observed in Fig. 4, the effective stress under both boundary conditions decreases with the pore pressure increase; with the helium pressure decrease, the increase in the effective stress under the USB condition is slower

**Fig. 4** Variation of helium permeability and effective stress with pore pressure change under two boundary conditions



than that under the CSB condition. That is due to the fact that the uniaxial strain condition experiments will reduce the lateral stress to ensure the zero lateral strain, leading to a slower increment of effective lateral stress. Figure 4 also shows the curves of helium gas permeability under both boundary conditions behaving in the same trend; they both decrease with the pore pressure drawdown. With pore pressure decreasing from 4.1 to 0.16 MPa, the permeability decreases from ~9 to ~2.72 × 10<sup>-16</sup> D under the CSB condition and ~9.17 to ~2.93 × 10<sup>-16</sup> D under the USB condition. The helium permeability under the CSB condition is found to be lower than that under the USB condition, which well correlates with the effective stress change under the two boundaries. Additionally, the permeability curves measured under the two boundaries do not show a rebound in the low-pressure stage, nor does it show a linear decay with the decrease in pressure. The reason is simply because the slip flow, also known as Klinkenberg effect, becomes more significant as the pressure drawdown, which will positively affect the apparent permeability in porous media in low-pore-pressure stage during gas depletion (Clarkson et al. 2011; Wang et al. 2014). However, the influence of Klinkenberg effect on permeability is not enough to alter the permeability decay trend in the low-pressure stage, which implies that the helium gas permeability evolution is mainly controlled by the effective stress change in the tested coals.

### 5.4 Sorbing Gas (CH<sub>4</sub> and CO<sub>2</sub>) Permeability

Figure 5 shows the measured permeability values for the sorbing gas under the CSB and USB conditions. It shows that the profile of sorbing gas permeability values under both boundary conditions has similar behavior; the gas permeability initially declines and then starts to increase with the pressure depletion. For the CH<sub>4</sub> permeability change under the USB condition, the permeability decreases from ~3.41 to ~1.29 × 10<sup>-16</sup> D with pore pressure decreasing from 4.07 to 0.87 MPa, and it increases to ~1.49 × 10<sup>-16</sup> D with the pressure decreases to 0.22 MPa. As is well known, CBM production from coal reduces gas pressure in the fracture network. And consequently, the decrease in the fracture pressure increases the effective stress in coal. As the fracture pressure drops below the gas pressure in pores of matrix, the adsorbed gas will desorb/diffuse from coal matrix to fractures, resulting in the shrinkage of coal matrix. The increased effective stress will lead to fracture compaction and aperture width decrease, while the matrix shrinkage increases the fracture aperture width. Thus, the variation of inherent permeability in coal is controlled by the net

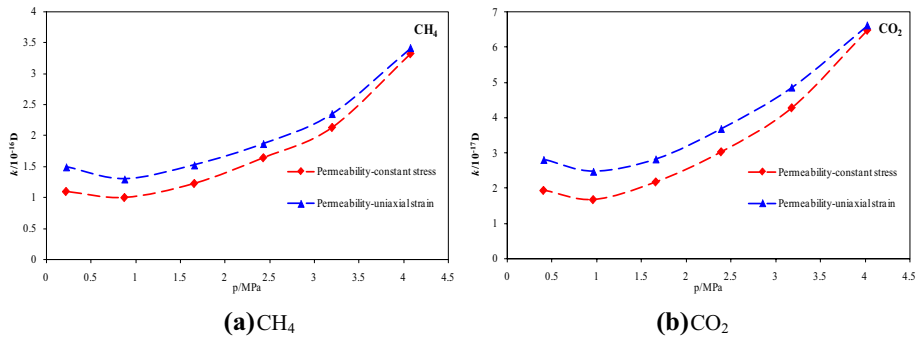


**Fig. 5** Change curves of gas permeability with pore pressure for CH<sub>4</sub> and CO<sub>2</sub>

influence of the two dual competing mechanisms. However, the result of both field tests and laboratory observations are apparent permeability, which incorporates not only the two dual competing mechanism effective stress and matrix shrinkage, but also the influence of gas slippage phenomenon which becomes more pronounced as the pore pressure decreases.

In Fig. 5, it shows that gas permeability obtained with the CSB condition decays at a slower rate than that with the USB condition during gas depletion. To maintain the uniaxial strain condition, the confining stress will be reduced with the pore pressure drawdown to ensure the zero lateral strain. The lateral stress remains constant under the CSB condition during the whole test procedure. Therefore, the CSB experiments will experience a faster increment of effective lateral stress than the USB experiments, which will result in a stronger mechanical deformation in coal, thus leading to faster permeability decay under the CSB condition.

Additionally, the permeability values of sorbing gases obtained under two boundaries have a greater difference than that of non-sorbing gas. It implies that the matrix shrinkage effect on permeability evolution is very sensitive to the boundary condition implemented on coal. This also demonstrates that setting suitable boundary condition in laboratory tests is critical to accurately determining permeability of coal.

## 5.5 Klinkenberg Effect on Permeability Change in the Tested Coal

Based on the previous studies, Klinkenberg effect becomes more significant with the reduction of pore pressure in gas depletion (Clarkson et al. 2011). The mean free path of gas molecule is far less than the coal fracture aperture at the high-pressure stage, and correspondingly, molecule–molecule collisions are more frequent than the molecule–solid wall collisions. Therefore, the gas slippage is not considered as the main cause for the apparent permeability variation at high-pressure stage. The helium is considered as the non-sorbing gas because it has a very low adsorption capacity on coal, and the matrix swelling induced and permeability change caused by helium depletion from coal are regarded as negligible. Thus, the apparent permeability alteration during helium flow through coal can be partly attributed to mechanical compaction related to the effective stress change and partly attributed to gas slippage in micropores in coal. However, Fig. 4 shows that the helium permeability curves did not show the rebound in low-pressure region, indicating that the effective stress is the main controlling factor of helium gas permeability evolution in the coal tested in the current study.

The Knudsen number characterizes the intensity of Klinkenberg effect, expressed by Eq. (3) (Wang et al. 2014):

$$k_n = \frac{\lambda}{w_{\text{pore}}} \quad (3)$$

where  $k_n$  indicates Knudsen number,  $\lambda$  indicates the mean free path of gas molecules and  $w_{\text{pore}}$  indicates pore width. Under the same conditions (pore size, pressure, temperature and so on), the Klinkenberg effects of different gases are also different, and the mean free paths  $\lambda$  of different gases are ranked as  $\lambda_{\text{He}} > \lambda_{\text{CO}_2} > \lambda_{\text{CH}_4}$  (Liu 2012). Thus, the Klinkenberg effect of  $\text{CH}_4$  and  $\text{CO}_2$  on permeability behavior should be less than that of helium. As observed in Fig. 4, the Klinkenberg effect failed to inhibit the permeability decay induced by pressure depletion. Therefore, the Klinkenberg effect of  $\text{CH}_4$  or  $\text{CO}_2$  flow in the same coal core will not eliminate the decline in permeability. And it is inferred that the permeability 'rebound' of sorbing gas may be mainly caused by the shrinkage strain related to high-intensity gas desorption from coal matrix.

## 5.6 Mechanism of Permeability 'Rebound' Behavior for the Sorbing Gas

At the initial stage, the sorbing gas permeability decreases with gas depletion, which is attributed to the effective stress increase. Although the matrix shrinkage also occurs in high-pressure region, the amount of desorbed gas from coal matrix is insignificant, which will not lead to much shrinkage strain in coal matrix and will not remarkably affect the permeability behavior. On the other side, the decrease in the pore pressure of fracture network increases the effective stress in coal, which will compress the fracture and narrow the gas flow channels, lowering the gas permeability in coal. Simultaneously, gas slippage is not prevailing in the high-pore-pressure stage, and its influence on permeability variation is negligible (Wang et al. 2014; Wang and Liu 2018). Therefore, at the high-pressure stage of gas depletion, the effective stress is the dominate factor controlling the gas permeability variation.

As the pore pressure keeps decreasing, the matrix will desorb more gas, and this desorption will induce a stronger shrinkage deformation of the coal matrix. The matrix shrinkage effect will expand the aperture of the fracture and increase the permeability. Thus, with the gas pressure depletion, the matrix shrinkage effect will make a gradual contribution to increase the permeability of coal, and at the low-pressure stage, the matrix shrinkage will become the main factor controlling the permeability change. Strains induced by the variation of effective stress and matrix shrinkage alter the inherent pore structure of coal, and these deformations change the inherent permeability of coal. Figure 6 displays the mechanism of inherent permeability change for the sorbing gas depletion in coal.

Gas slippage effect is such a phenomenon showing that the measured gas permeability (apparent permeability) is potentially higher than the pure liquid permeability (inherent permeability) in specific flow regime (Wang et al. 2015). As the pore pressure decreases, gas slippage effect becomes more significant. Although gas slippage will not change the inherent coal structure and permeability, it will improve the apparent permeability, especially in flows in medium with well-developed micropores at a low-pressure region. Therefore, the combined effect of matrix shrinkage and gas slippage induces the apparent permeability enhancement; when the combined effect exceeds the mechanical compression effect on permeability change, the 'permeability rebound' will occur, as observed in Fig. 5. The

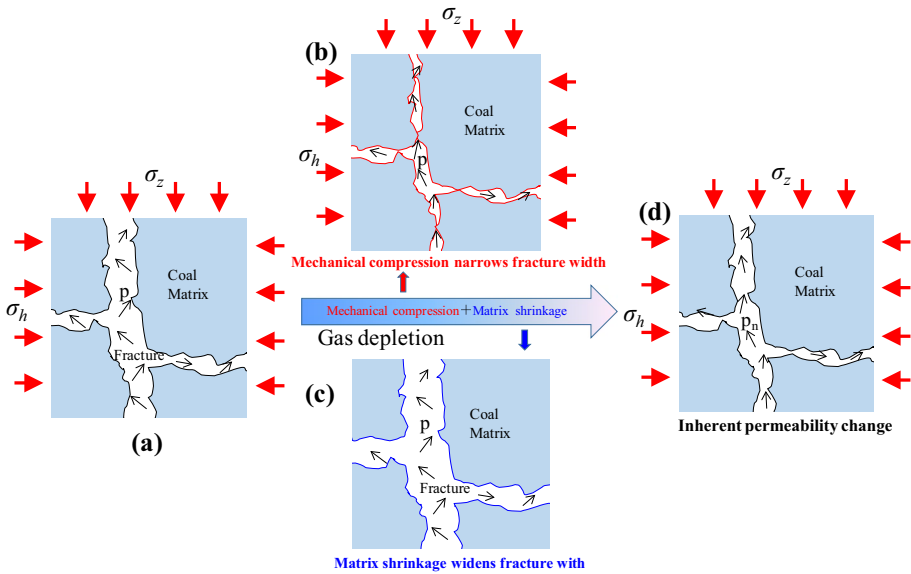


**Fig. 6** Schematic of inherent permeability change induced by coal mass deformation with sorbing gas depletion (**a** coal mass at initial time, **b** volumetric strain purely induced by mechanical compression, **c** volumetric strain purely induced by gas desorption, **d** coal mass at specified gas pressure; ‘ $\sigma_z$ ’ and ‘ $\sigma_h$ ’ refer to the vertical and horizontal stress, respectively)

mechanism of ‘permeability rebound’ for the sorbing gas depletion in coal is shown in Fig. 7.

Additionally, comparing the permeability curves of  $\text{CH}_4$  and  $\text{CO}_2$ , it can be observed that the ‘permeability rebound’ of the  $\text{CH}_4$  permeability curve is comparatively smaller than that of  $\text{CO}_2$ . This might be due to the fact that the  $\text{CO}_2$  sorption capacity on coal is higher than that of  $\text{CH}_4$  in the same coals, which will lead to a larger amount of  $\text{CO}_2$  desorption, incurring a greater shrinkage deformation and permeability rebound in coal.

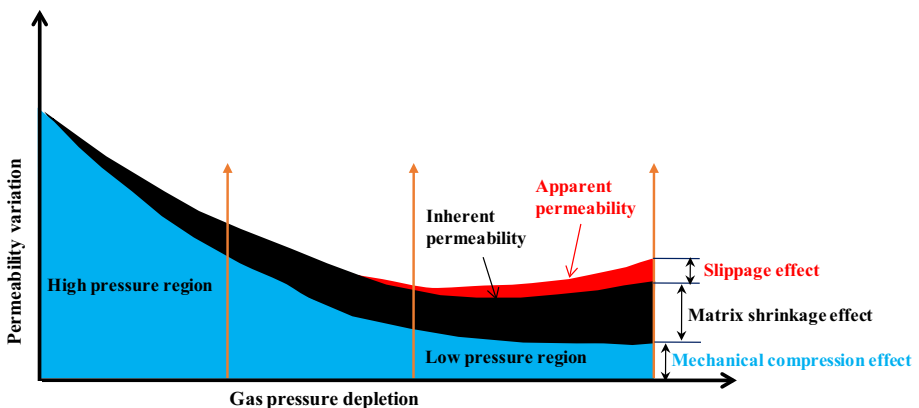


**Fig. 7** Mechanism of permeability variation with gas depletion

However, both  $\text{CH}_4$  and  $\text{CO}_2$  permeabilities do not recover to its original values. This might be attributed to the inner coal structure and the fact that the matrix shrinkage strain is fairly smaller than the mechanical compression strain induced by the effective stress increasing during pore pressure depletion in coal.

## 5.7 Implication for the Overall CBM Production Process

Gas permeability is one of the key parameters affecting the gas flow behavior in coal seam (Fan and Liu 2019; Yang and Liu 2019). A comprehensive understanding of the permeability evolution mechanism and the key factors that dominate the gas production is of basic significance for planning and projecting CBM recovery. In terms of estimating CBM production, most studies in this field support that the overall CBM production is mainly dominated by fracture permeability. Those studies have given tremendous attention to coal reservoir fracturing for improving gas deliverability in the reservoir fracture (Liu et al. 2012; Pan et al. 2012). However, the gas flow in coal is a multi-scale and multi-mechanism process. At different pore pressure stages, the fracture and matrix flow parameters, such as permeability of coal fracture, gas diffusion coefficient and desorption rate in coal matrix, are different, and the gas flow behavior is also different, which will lead to the variation in gas production rate. Who dominates the gas production during the whole CBM recovery life, fracture flow dominates or a dynamic mechanism dominates?

Based on the gas transport mechanism in dual-porosity coal, at the initial stage, gas production is mainly controlled by the original free gas amount stored in fracture space and the gas transport flux in fracture system which dominated by fracture permeability; and at this stage, the gas desorbed amount from the matrix is quite limited and has little effect on gas production (Liu et al. 2018b; Wang et al. 2018; Pillalamarry et al. 2011). As gas depletion continues, free gas is quickly depleted, and the adsorbed gas within coal matrix is gradually desorbed and released, providing a gas source for the fractures. During this period, the gas release rate from coal matrix determines the gas flow flux in fractures and ultimately controls the well gas production rate, as shown in Fig. 8. The matrix parameters, such as the diffusion parameters and matrix size, affect the gas desorption and transport flux with the coal matrix, and thus the strength of the gas source for the fracture flow, and matrix starts to play an increasing role in gas production. Besides, the amount of desorbed gas from the matrix is directly proportional to the matrix shrinkage deformation of the coal. Thus, with the pore pressure depletion, a higher gas flux in the matrix will promote the ‘permeability rebound’ and consequently accelerate the fracture flow flux.

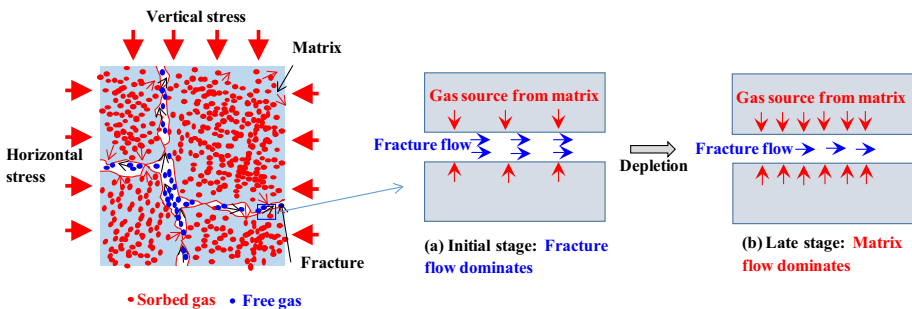


Fig. 8 Dynamic control factors of gas production rate



In summary, the mechanism of CBM production is dynamically varying in accordance with gas depletion: At the initial stage of gas production, effective stress dominates permeability evolution and fracture permeability controls the fracture flow flux and then the gas production rate; at the later stage of gas production, the matrix shrinkage effect and gas slippage effect control the ‘permeability rebound,’ and matrix flow parameters dominate the rate of gas production, as shown in Fig. 9. This reminds us that only focusing on coal fracturing is still not enough for ECBM operation and it is more important to stimulate the gas desorption from the coal matrix, so that it can enhance the gas production throughout the whole CBM well lifecycle.

## 6 Conclusion

Theoretical models and a series of pulse-decay experiments on gas permeability of low-permeability coal samples under different stressed controlled boundary conditions have been reported. Results show that the permeability variation behavior of the studied coal is stress boundary-dependent and is collectively affected by the effective stress and the matrix desorption process. Based on the current study, the following conclusions are made:

1. For the pulse-decay method, the effect of the matrix gas desorption can be clearly observed from the pressure response curves. The time required to approach the equilibrium increases with the decrease in the injection pressure and the equilibrium time for the  $\text{CH}_4$  and  $\text{CO}_2$  gas pressure is generally higher than that for helium. This indicates that sorbing gases tested here flow slower than helium under similar conditions. It also indicates that coal permeability is a gas type-dependent property.
2. Helium permeability characteristics under both boundary conditions vary in the same trend, and permeability under the constant stress condition is found to be lower than that under the uniaxial strain condition. The helium permeability curves do not rebound, nor does it decay linearly with the decrease in pressure. The reason is simply because the Klinkenberg effect becomes more significant in low-pore-pressure stage and posi-

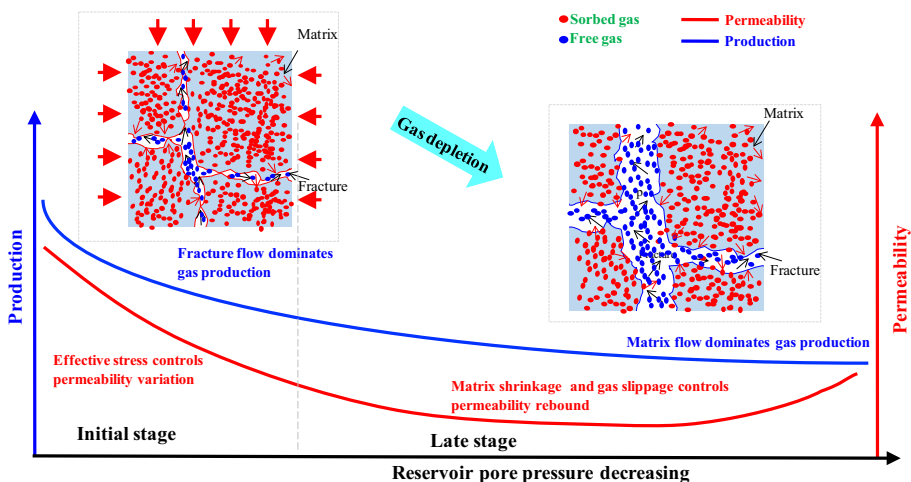


Fig. 9 Dynamic mechanism of CBM production with gas depletion

- tively affects the apparent permeability in coal. However, Klinkenberg effect does not inhibit the permeability decay with continuous pressure depletion, which implies that the helium permeability evolution is mainly controlled by the effective stress change in the tested coals.
3. For the sorbing gas (CH<sub>4</sub> and CO<sub>2</sub>), the permeability profile under both boundary conditions behaves somewhat similarly; it initially declines with the pressure depletion and then starts to increase. Due to the larger sorption capacity of CO<sub>2</sub> in coal, the permeability 'rebound' of CO<sub>2</sub> permeability is comparatively stronger than that of CH<sub>4</sub>. With the comparison of permeability behavior of non-sorbing/sorbing gas in low-pressure stage, the permeability 'rebound' of sorbing gas is mainly attributed to the matrix shrinkage caused by high-intensity desorption in coal.
  4. The CBM production mechanism varies dynamically as a function of gas depletion: At the initial stage, the effective stress dominates the permeability evolution while the fracture permeability controls gas production. At the late stage, the matrix shrinkage and gas slippage control the 'permeability rebound' behavior while the matrix flow dominates gas production. This reveals that stimulating the gas flow flux within coal matrix could be more important to enhance the overall CBM production.

**Acknowledgements** This work was supported by the National Key R&D Program of China (No. 2017YFC0804202), National Science and Technology Major Project (2016ZX05045001-005) and Postdoctoral Science Foundation Project Funded by State Key Laboratory of Coal Mine Disaster Dynamics and Control (2011DA105287-BH201901), which are all greatly appreciated.

## References

- Brace, W., Walsh, J., Frangos, W.: Permeability of granite under high pressure. *J Geophys Res* **73**(6), 2225–2236 (1968)
- Chen, Z., Liu, J., Pan, Z., et al.: Influence of the efficient and sorption-induced strain on the evolution of coal permeability: model development and analysis. *Int J Green Gas Con* **8**, 101–110 (2012)
- Chen, D., Pan, Z., Shi, J., et al.: A novel approach for modeling coal permeability during transition from elastic to post-failure state using a modified logistic growth function. *Int J Coal Geol* **163**, 132–139 (2016)
- Cheng, Y., Pan, Z.: Reservoir properties of Chinese tectonic coal: a review. *Fuel* **260**, 116350 (2020)
- Clarkson, C., Nobakht, M., Kaviani, D., et al.: Production analysis of tight gas and shale gas reservoirs using the dynamic-slippage concept. *SPE J* **17**(1), 230–242 (2012)
- Connell, L.D.: A new interpretation of the response of coal permeability to changes in pore pressure, stress and matrix shrinkage. *Int J Coal Geol* **162**, 169–182 (2016)
- Crosdale, P., Beamish, B., Valix, M.: Coalbed methane sorption related to coal composition. *Int J Coal Geol* **35**, 147–158 (1998)
- Cui, X., Bustin, R.: Volumetric strain associated with methane desorption and its impact on coalbed gas production from deep coal seams. *AAPG Bull.* **89**(9), 1181–1202 (2005)
- Durucan, S., Edwards, J.: The effects of stress and fracturing on permeability of coal. *Mining Sci Technol* **3**, 205–216 (1986)
- Durucan, S., Ahsan, M., Shi, J., et al.: Two phase relative permeabilities for gas and water in selected European coals. *Fuel* **134**, 226–236 (2014)
- Fan, L., Liu, S.: Fluid-dependent shear slip behaviors of coal fractures and their implications on fracture frictional strength reduction and permeability evolutions. *Int J Coal Geol* **212**, 103235 (2019)
- Fan, J., Liu, P., Li, J., Jiang, D.: A coupled methane/air flow model for coal gas drainage: model development and finite-difference solution. *Process Saf Environ Prot* **141**, 288–304 (2020)
- Feng, R., Harpalani, S., Pandey, R.: Laboratory measurement of stress-dependent coal permeability using pulse-decay technique and flow modeling with gas depletion. *Fuel* **177**(1), 76–86 (2016)

- Feng, R., Harpalani, S., Pandey, R.: Evaluation of various pulse-decay laboratory permeability measurement techniques for highly stressed coals. *Rock Mech Rock Eng* **50**, 297–308 (2017)
- Feng, R., Chen, S., Bryant, S., et al.: Stress-dependent permeability measurement techniques for unconventional gas reservoirs: review, evaluation, and application. *Fuel* **256**, 115987 (2019)
- Gray, I.: Reservoir engineering in coal seams: Part 1. The physical process of gas storage and movement in coal seams. *SPE Reservoir Eng* **2**(1), 28–34 (1987)
- Harpalani, S., Chen, G.: Influence of gas production induced volumetric strain on permeability of coal. *Geotech Geol Eng* **15**(4), 303–325 (1997)
- Harpalani, S., McPherson, M.: Effect of stress on permeability of coal. *Q Rev Methane Coal Seams Technol* **3**, 23–28 (1985)
- Harpalani, S., Schraufnagel, R.: Shrinkage of coal matrix with release of gas and its impact on permeability of coal. *Fuel* **69**(5), 551–556 (1990)
- Levine, J.: Model study of the influence of matrix shrinkage on absolute permeability of coal bed reservoirs. In: Gayer, R., Harris, I. (eds.) *Coalbed methane and coal geology*: Geological Society (London), pp. 197–212. Special Publication (1996)
- Liu, S.: Estimation of different coal compressibilities of coalbed methane reservoirs under replicated in situ condition. Southern Illinois University Carbondale, USA (2012)
- Liu, S., Harpalani, S.: A new theoretical approach to model sorption induced coal shrinkage and swelling. *AAPG Bull.* **97**(7), 1033–1049 (2013)
- Liu, S., Harpalani, S.: Evaluation of in situ stress changes with gas depletion of coalbed methane reservoirs. *J Geophys Res Solid Earth* **119**(8), 6263–6276 (2014)
- Liu, H., Rutqvist, J.: A new coal-permeability model: internal swelling stress and fracture–matrix interaction. *Transp Porous Media* **82**(1), 157–171 (2010)
- Liu, J., Chen, Z., Elsworth, D., et al.: Evaluation of stress-controlled coal swelling processes. *Int J Coal Geol* **83**(4), 446–455 (2010)
- Liu, S., Harpalani, S., Pillalamarry, M.: Laboratory measurement and modeling of coal permeability with continued methane production: Part 2 – Modeling results. *Fuel* **94**, 117–124 (2012)
- Liu, S., Wang, Y., Harpalani, S.: Anisotropy characteristics of coal shrinkage/swelling and its impact on coal permeability evolution with CO<sub>2</sub> injection. *Greenhouse Gas Sci Technol* **6**(5), 615–632 (2016)
- Liu, P., Qin, Y., Liu, S., et al.: Non-linear gas desorption and transport behaviors in coal matrix: experiments and numerical modeling. *Fuel* **214**, 1–13 (2018a)
- Liu, P., Qin, Y., Liu, S., et al.: Numerical modeling of gas flow in coal using a modified dual-porosity model: a multi-mechanistic approach and finite difference method. *Rock Mech Rock Eng* **51**, 2863–2880 (2018b)
- Liu, A., Liu, S., Hou, X., Liu, P.: Transient gas diffusivity evaluation and modeling for methane and helium in coal. *Int J Heat Mass Transf* **159**, 120091 (2020)
- Liu, A., Liu, P., Shimin, L.: Gas diffusion coefficient estimation of coal: a dimensionless numerical method and its experimental validation. *Int J Heat Mass Transf* **162**, 120336 (2020b)
- Liu, P., Liu, A., Zhong, F., et al.: Pore/fracture structure and gas permeability alterations induced by ultrasound treatment in coal and its application to enhanced coalbed methane recovery. *J Petrol Sci Eng* **205**, 108862 (2021)
- Ma, Q., Harpalani, S., Liu, S.: A simplified permeability model for coalbed methane reservoirs based on matchstick strain and constant volume theory. *Int J Coal Geol* **85**, 43–48 (2011)
- Mitra, A.: Laboratory investigation of coal permeability under replicated in situ stress regime. Southern Illinois University at Carbondale, Ann Arbor (2010)
- Mitra, A., Harpalani, S., Liu, S.: Laboratory measurement and modeling of coal permeability with continued methane production: Part 1–Laboratory results. *Fuel* **94**, 110–116 (2012)
- Moore, T.A.: Coalbed methane: a review. *Int J Coal Geol* **101**(101), 36–81 (2012)
- Niu, Y., Mostaghimi, P., Shikhov, I., et al.: Coal permeability: gas slippage linked to permeability rebound. *Fuel* **215**, 844–852 (2018)
- Palmer, I.: Permeability changes in coal: analytical modeling. *Int J Coal Geol* **77**(1), 119–126 (2009)
- Palmer, I.: Coalbed methane completions: a world view. *Int J Coal Geol* **82**(3), 184–195 (2010)
- Palmer, I., Mansoori, J.: How permeability depends on stress and pore pressure in coalbeds: a new model. In: *SPE annual technical conference and exhibition*. Soc Pet Eng **1**(06), 539–544 (1996)
- Pan, Z., Connell, L.D.: Modelling of anisotropic coal swelling and its impact on permeability behaviour for primary and enhanced coalbed methane recovery. *Int J Coal Geol* **85**, 257–267 (2011)
- Pan, Z., Connell, L.D.: Modelling permeability for coal reservoirs: a review of analytical models and testing data. *Int J Coal Geol* **92**, 1–44 (2012)
- Pan, Z., Connell, L.D., Camilleri, M.: Laboratory characterisation of coal reservoir permeability for primary and enhanced coalbed methane recovery. *Int J Coal Geol* **82**, 252–261 (2010)

- Pekot, L.J., Reeves, S.R.: Modeling the effects of matrix shrinkage and differential swelling on coalbed methane recovery and carbon sequestration. Proceedings of the 2003 International Coalbed Methane Symposium. University of Alabama (2003)
- Peng, Y., Liu, J., Pan, Z., et al.: Impact of coal matrix strains on the evolution of permeability. *Fuel* **189**(1), 270–283 (2017)
- Perera, M., Ranjith, P., Choi, S., et al.: Investigation of temperature effect on permeability of naturally fractured black coal for carbon dioxide movement: an experimental and numerical study. *Fuel* **94**, 596–605 (2012)
- Pillalamarry, M., Harpalani, S., Liu, S.: Gas diffusion behavior of coal and its impact on production from coalbed methane reservoirs. *Int J Coal Geol* **86**, 342–348 (2011)
- Pini, R., Ottiger, S., Burlini, L., et al.: Role of adsorption and swelling on the dynamics of gas injection in coal. *J Geophys Res Solid Earth* **114**, B04203 (2009)
- Ritter, D., Vinson, D., Barnhart, E., Akob, D., et al.: Enhanced microbial coalbed methane generation: a review of research, commercial activity, and remaining challenges. *Int J Coal Geol* **146**, 28–41 (2015)
- Robertson, E.P.: Measurement and modeling of sorption-induced strain and permeability changes in coal. Ph.D. dissertation, Colorado School of Mines, Golden, Colorado (2005)
- Sawyer, W.K., Paul, G.W., Schraufnagel, R.A.: Development and application of a 3-D coalbed simulator. In: Annual technical meeting. Petroleum Society of Canada (1990)
- Seidle, J.P., Jeansonne, M.W., Erickson, D.J.: Application of matchstick geometry to stress dependent permeability in coals. In: SPE rocky mountain regional meeting. Society of Petroleum Engineers (1992)
- Shi, J.Q., Durucan, S.: Drawdown induced changes in permeability of coalbeds: a new interpretation of the reservoir response to primary recovery. *Transp Porous Media* **56**(1), 1–16 (2004)
- Shi, J.Q., Durucan, S.: A model for changes in coalbed permeability during primary and enhanced methane recovery. *SPE Reservoir Eval. Eng.* **8**(04), 291–299 (2005)
- Wang, Y., Liu, S.: Estimation of pressure-dependent diffusive permeability of coal using methane diffusion coefficient: laboratory measurements and modeling. *Energy Fuels* **30**(11), 8968–8976 (2016)
- Wang, G., Ren, T., Wang, K., et al.: Improved apparent permeability models of gas flow in coal with Klinkenberg effect. *Fuel* **128**, 53–61 (2014)
- Wang, Y., Liu, S., Elsworth, D.: Laboratory investigations of gas flow behaviors in tight anthracite and evaluation of different pulse-decay methods on permeability estimation. *Int J Coal Geol* **149**, 118–128 (2015)
- Wang, Y., Liu, S., Zhao, Y.: Modeling of permeability for ultra-tight coal and shale matrix: a multi-mechanistic flow approach. *Fuel* **232**, 60–70 (2018)
- Wu, T., Pan, Z., Connell, L.D., et al.: Apparent gas permeability behavior in the near critical region for real gases. *J Nat Gas Sci Egn* **77**, 103245 (2020)
- Yang, Y., Liu, S.: Estimation and modeling of pressure-dependent gas diffusion coefficient for coal: a fractal theory-based approach. *Fuel* **253**, 588–606 (2019)
- Zang, J., Ge, Y., Wang, K.: The principal permeability tensor of inclined coalbeds during pore pressure depletion under uniaxial strain conditions: developing a mathematical model, evaluating the influences of featured parameters, and upscaling for CBM recovery. *J Nat Gas Sci Egn* **74**, 103099 (2020)
- Zhang, X., Ranjith, P., Perera, M., et al.: Gas transportation and enhanced coalbed methane recovery processes in deep coal seams: a review. *Energy Fuels* **30**, 8832–8849 (2016)

**Publisher's Note** Springer Nature remains neutral with regard to jurisdictional claims in published maps and institutional affiliations.